B. Dubus
Institut d'Electronique, de Microélectronique
et de Nanotechnologie,
UMR CNRS 8520,
Cité Scientifique,
Villeneuve d'Ascq Cedex 59652, France
e-mail: bertrand.dubus@isen.fr

N. Swinteck
Department of Materials
Science and Engineering,
University of Arizona,
Tucson, AZ 85721
e-mail: swinteck@email.arizona.edu

K. Muralidharan
Department of Materials
Science and Engineering,
University of Arizona,
Tucson, AZ 85721
e-mail: krishna@email.arizona.edu

J. O. Vasseur
Institut d'Electronique de,
Microélectronique et de Nanotechnologie,
UMR CNRS 8520,
Cité Scientifique,
Villeneuve d'Ascq Cedex 59652, France
e-mail: jerome.vasseur@univ-lille1.fr

P. A. Deymier
Department of Materials
Science and Engineering,
University of Arizona,
Tucson, AZ 85721
e-mail: deymier@email.arizona.edu

Nonlinear Phonon Modes in Second-Order Anharmonic Coupled Monoatomic Chains

We have used multiple-time-scales perturbation theory as well as the numerical methods of molecular dynamics and spectral energy density (SED) to investigate the phonon band structure of a two-chain model with second-order anharmonic interactions. We show that when one chain is linear and the other is nonlinear, the two-chain model exhibits a nonlinear resonance near a critical wave number due to mode self-interaction. The nonlinear resonance enables wave number-dependent interband energy transfer. We have also shown that there exist nonlinear modes within the spectral gap separating the lower and upper branches of the phonon band structure. These modes result from three phonon interactions between a phonon belonging to the nonlinear branch and two phonons lying on the lower branch. This phenomenon offers a mechanism for phonon splitting.
[DOI: 10.1115/1.4033457]

1 Introduction

Coupled nonlinear and linear mechanical systems have recently received attention for their application in targeted energy transfer, whereby undesirable mechanical energy is directed irreversibly from a linear system to a nonlinear system [1]. Targeted energy transfer involves nonlinear resonances between the linear and nonlinear systems. So far, linear–nonlinear coupled systems that have been investigated focused on systems with a small number of degrees-of-freedom [2–4] or linear systems with small number of degrees-of-freedom coupled to a nonlinear attachments or absorber [5,6]. Systems with multiple degrees-of-freedom have been addressed by considering finite linear chains with nonlinear end attachments [7,8]. In this context, we report on a detailed study of the dynamics of coupled linear–nonlinear discrete systems with an infinite number of degrees-of-freedom. More specifically, we address the elastic vibrational propagative modes supported by a model of two coupled discrete infinite one-dimensional mass-spring chains with second-order nonlinearity. We contrast the behavior of coupled linear–nonlinear chains to that of the linear–linear and nonlinear–nonlinear two-chain models. It is very well known that the phonon band structure of the linear two-chain model possess an asymmetric and a symmetric bands. We show that irreversible energy transfer is achieved between the symmetric and the asymmetric bands of the linear–nonlinear coupled chain model. This transfer is associated with an interband resonance resulting from the quadratic nonlinearity. The nonlinear–nonlinear two-chain model does not possess such a resonance. We have also identified three-phonon processes that lead to the creation of a third band in the phonon band structure of the linear–nonlinear two-chain model. This nonlinear band bridges the symmetric and asymmetric bands. The three-phonon process may be used to split a phonon into a pair of phonons offering an avenue to realizing a source of correlated phonons. The emitted pair of phonons is located in the lower branch of the band structure and they have a combined frequency and wave number equal to the frequency and wave number of the split nonlinear phonon. From the point of view of phononic systems that are isomorphic to the present nonlinear two-chain model, this work has relevance to the study of a variety of low-dimensionality phononic structures or nanostructures such as elastic modes in coupled granular chains [9]. The study of nonlinear two-chain models is also relevant to the study of phonons in two-leg ladders [10]. Nonlinear vibrational modes in nonlinear discrete two-chain models have also been used to describe the thermal properties of DNA [11].

Contributed by the Technical Committee on Vibration and Sound of ASME for publication in the JOURNAL OF VIBRATION AND ACOUSTICS. Manuscript received August 20, 2015; final manuscript received April 7, 2016; published online May 25, 2016. Assoc. Editor: Mohammed Daqaq.

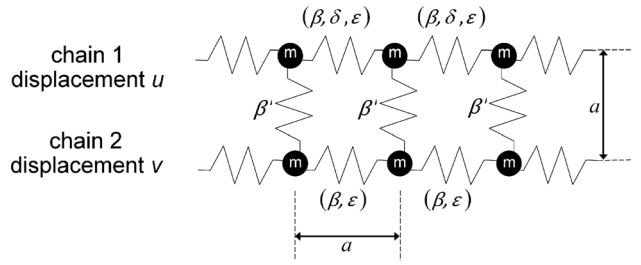

Fig. 1 Schematic illustration of the two coupled infinite atomic chains made of identical atoms of mass *m* with a lattice parameter *a*. β would correspond to the stiffness of the spring linking atoms in the two horizontal chains if these springs were linear. A degree of nonlinearity can be introduced inside the model via parameters δ and ε (see text for definition). β' is the stiffness of the linear spring connecting together atoms *n* in the two horizontal chains.

The paper is organized as follows. We introduce the nonlinear two-chain model in Sec. 2 and recall the basic principles of the multiple-time-scales perturbation theory. In Sec. 3, this theory is employed to reveal the nonlinear phonon resonance and the energy transfer in the vicinity of the resonance in the two-chain model that arise from phonon self-interaction. The perturbation theory is extended, in Sec. 4, to the investigation of three-phonon scattering processes and the identification of nonlinear vibrational modes. In Sec. 5, we subsequently use the method of molecular dynamics and the SED method to calculate the complete band structure of the linear–nonlinear and the nonlinear–nonlinear two-chain models and confirm the analytical predictions. Specifically, we observe the existence of nonlinear modes resulting from three-phonon processes inside the gap separating the usual lower and upper dispersion branches of the two-chain system. Finally, the work is summarized and conclusions are drawn in Sec. 6.

2 Model and Methods

2.1 Model Systems. For the sake of generality, we consider the case of two parallel infinite chains of lattice parameter, a, made of identical atoms of mass m. The two chains are coupled together with a spring of linear stiffness, β'. Each atomic site "n" in chain 1 (resp. chain 2) is characterized by a displacement, u_n (resp. v_n). We assume that the model is limited to first nearest neighbor interactions (see Fig. 1).

The two parallel chains are supposed to be anharmonic and the interaction forces between two adjacent masses n and $n+1$ are taken as the sum of a linear and a second-order terms

$$F^{(1)}_{n,n+1} = \beta(u_{n+1} - u_n) + \delta\varepsilon(u_{n+1} - u_n)^2 \tag{1}$$

in chain 1 and as

$$F^{(2)}_{n,n+1} = \beta(v_{n+1} - v_n) + \varepsilon(v_{n+1} - v_n)^2 \tag{2}$$

in chain 2. In Eqs. (1) and (2), the parameter ε characterizes the strength of the nonlinearity in the springs connecting the masses constituting the two chains and the parameter δ that can take the values 0 or 1 is used to switch on and off the nonlinearity of chain 1 with respect to that of chain 2. If $\delta = 0$, chain 1 is harmonic with springs of linear stiffness β while chain 2 remains anharmonic. This case is named subsequently the linear–nonlinear two-chain model. When $\delta = 1$, both chains possess the same level of anharmonicity, this is denoted as the nonlinear–nonlinear system. Consequently, the equations of motion for atomic sites n in chains 1 and 2 are given as

$$\begin{cases} \dfrac{\partial^2 u_n}{\partial t^2} - \dfrac{\Omega^2}{4}(u_{n+1} - 2u_n + u_{n-1}) - \Omega'^2(v_n - u_n) \\ \qquad - \dfrac{\delta\varepsilon}{m}\left[(u_{n+1} - u_n)^2 - (u_n - u_{n-1})^2\right] = 0 \\ \dfrac{\partial^2 v_n}{\partial t^2} - \dfrac{\Omega^2}{4}(v_{n+1} - 2v_n + v_{n-1}) - \Omega'^2(u_n - v_n) \\ \qquad - \dfrac{\varepsilon}{m}\left[(v_{n+1} - v_n)^2 - (v_n - v_{n-1})^2\right] = 0 \end{cases} \tag{3}$$

where $\Omega^2 = 4\beta/m$ and $\Omega'^2 = \beta'/m$. The third terms in the left-hand side (LHS) of these equations are associated with the linear springs connecting mechanically the chains.

2.2 Multiple-Time-Scales Perturbation Method. Nowadays, the multiple-time-scales perturbation theory (MTSPT) for differential equations is a very popular method to approximate solutions of weakly nonlinear differential equations. Several implementations of this method were proposed in various fields of mathematics, mechanics, and physics [12–18]. Moreover, Khoo and Wang [19] have shown that the MTSPT is a reliable theoretical tool for studying the lattice dynamics of an anharmonic crystal. More recently, Swinteck et al. [20] applied successfully the MTSPT, as described in Ref. [19], for solving propagation equations in a quadratically nonlinear monoatomic chain of infinite extent. Consequently, we used the MTSPT for solving Eq. (3). For the sake of analytical simplicity, we treat ε as a perturbation and write the displacements u_n and v_n as second-order power series in the perturbation, namely

$$u_n(\tau_0, \tau_1, \tau_2) = u_n^{(0)}(\tau_0, \tau_1, \tau_2) + \varepsilon u_n^{(1)}(\tau_0, \tau_1, \tau_2) + \varepsilon^2 u_n^{(2)}(\tau_0, \tau_1, \tau_2) \tag{4}$$

$$v_n(\tau_0, \tau_1, \tau_2) = v_n^{(0)}(\tau_0, \tau_1, \tau_2) + \varepsilon v_n^{(1)}(\tau_0, \tau_1, \tau_2) + \varepsilon^2 v_n^{(2)}(\tau_0, \tau_1, \tau_2) \tag{5}$$

In Eqs. (4) and (5), $u_n^{(i)}$ and $v_n^{(i)}$ with $i = 0,\ 1,\ 2$ are displacement functions expressed to zeroth-order, first-order, and second-order in the perturbation, respectively. We have also replaced the single time variable, t, by three variables representing different time scales: $\tau_0 = t$, $\tau_1 = \varepsilon t = \varepsilon\tau_0$, and $\tau_2 = \varepsilon^2 t = \varepsilon^2\tau_0$. We can subsequently decompose Eqs. (4) and (5) into three pairs of equations: one to zeroth-order in ε, one to first-order in ε, and a third pair of equations to second-order in ε

$$\mathcal{O}(\varepsilon^0): \begin{cases} \dfrac{\partial^2 u_n^{(0)}}{\partial\tau_0^2} - \dfrac{\Omega^2}{4}\left(u_{n+1}^{(0)} - 2u_n^{(0)} + u_{n-1}^{(0)}\right) - \Omega'^2\left(v_n^{(0)} - u_n^{(0)}\right) = 0 & (6a) \\ \dfrac{\partial^2 v_n^{(0)}}{\partial\tau_0^2} - \dfrac{\Omega^2}{4}\left(v_{n+1}^{(0)} - 2v_n^{(0)} + v_{n-1}^{(0)}\right) + \Omega'^2\left(v_n^{(0)} - u_n^{(0)}\right) = 0 & (6b) \end{cases}$$

$$\mathcal{O}(\varepsilon^1): \begin{cases} \dfrac{\partial^2 u_n^{(1)}}{\partial\tau_0^2} - \dfrac{\Omega^2}{4}\left(u_{n+1}^{(1)} - 2u_n^{(1)} + u_{n-1}^{(1)}\right) - \Omega'^2\left(v_n^{(1)} - u_n^{(1)}\right) \\ = -2\dfrac{\partial^2 u_n^{(0)}}{\partial\tau_0\partial\tau_1} + \dfrac{\delta}{m}\left[\left(u_{n+1}^{(0)} - u_n^{(0)}\right)^2 - \left(u_n^{(0)} - u_{n-1}^{(0)}\right)^2\right] & (7a) \\ \dfrac{\partial^2 v_n^{(1)}}{\partial\tau_0^2} - \dfrac{\Omega^2}{4}\left(v_{n+1}^{(1)} - 2v_n^{(1)} + v_{n-1}^{(1)}\right) + \Omega'^2\left(v_n^{(1)} - u_n^{(1)}\right) \\ = -2\dfrac{\partial^2 v_n^{(0)}}{\partial\tau_0\partial\tau_1} + \dfrac{1}{m}\left[\left(v_{n+1}^{(0)} - v_n^{(0)}\right)^2 - \left(v_n^{(0)} - v_{n-1}^{(0)}\right)^2\right] & (7b) \end{cases}$$

$$\mathcal{O}(\varepsilon^2):\begin{cases}\dfrac{\partial^2 u_n^{(2)}}{\partial\tau_0^2}-\dfrac{\Omega^2}{4}\left(u_{n+1}^{(2)}-2u_n^{(2)}+u_{n-1}^{(2)}\right)-\Omega'^2\left(v_n^{(2)}-u_n^{(2)}\right)\\ =-2\dfrac{\partial^2 u_n^{(1)}}{\partial\tau_0\partial\tau_1}-2\dfrac{\partial^2 u_n^{(0)}}{\partial\tau_0\partial\tau_2}-2\dfrac{\partial^2 u_n^{(0)}}{\partial\tau_1^2}+\dfrac{2\delta}{m}\left[\begin{array}{l}\left(u_{n+1}^{(0)}-u_n^{(0)}\right)\left(u_{n+1}^{(1)}-u_n^{(1)}\right)\\ -\left(u_n^{(0)}-u_{n-1}^{(0)}\right)\left(u_n^{(1)}-u_{n-1}^{(1)}\right)\end{array}\right] \qquad (8a)\\ \dfrac{\partial^2 v_n^{(2)}}{\partial\tau_0^2}-\dfrac{\Omega^2}{4}\left(v_{n+1}^{(2)}-2v_n^{(2)}+v_{n-1}^{(2)}\right)+\Omega'^2\left(v_n^{(2)}-u_n^{(2)}\right)\\ =-2\dfrac{\partial^2 v_n^{(1)}}{\partial\tau_0\partial\tau_1}-2\dfrac{\partial^2 v_n^{(0)}}{\partial\tau_0\partial\tau_2}-2\dfrac{\partial^2 v_n^{(0)}}{\partial\tau_1^2}+\dfrac{2}{m}\left[\begin{array}{l}\left(v_{n+1}^{(0)}-v_n^{(0)}\right)\left(v_{n+1}^{(1)}-v_n^{(1)}\right)\\ -\left(v_n^{(0)}-v_{n-1}^{(0)}\right)\left(v_n^{(1)}-v_{n-1}^{(1)}\right)\end{array}\right] \qquad (8b)\end{cases}$$

In the course of the calculations, general solutions to Eq. (6) are first determined and then inserted into Eq. (7) to resolve for $u_n^{(1)}$ and $v_n^{(1)}$. Subsequently, solutions to Eqs. (6) and (7) allow solving for Eq. (8).

3 Self-Interaction

We first address the self-interaction of a vibrational mode (the effect of the lattice deformation on itself).

3.1 Zeroth-Order Solutions. One notes that Eq. (6) is strictly equivalent to the equations of motion when chains 1 and 2 are linear. The solutions of these equations can be written in the usual form

$$\begin{cases}u_n^{(0)}=A_0e^{ikna}e^{-i\omega\tau_0}\\ v_n^{(0)}=B_0e^{ikna}e^{-i\omega\tau_0}\end{cases} \qquad (9)$$

where A_0 and B_0 are constants to be determined with the initial conditions, k is the wave number of the propagation mode, ω is its pulsation, and a is the lattice parameter. Inserting these solutions into Eq. (6) leads to the following matrix equation:

$$\begin{pmatrix}\omega^2-\Omega^2\sin^2\left(\dfrac{ka}{2}\right)-\Omega'^2 & \Omega'^2\\ \Omega'^2 & \omega^2-\Omega^2\sin^2\left(\dfrac{ka}{2}\right)-\Omega'^2\end{pmatrix}\begin{pmatrix}A_0\\ B_0\end{pmatrix}=\begin{pmatrix}0\\ 0\end{pmatrix} \qquad (10)$$

Equation (10) admits two nontrivial solutions when the determinant of the matrix vanishes. These solutions are

$$\omega=\omega_0^-=\Omega\left|\sin\left(\frac{ka}{2}\right)\right| \qquad (11)$$

and

$$\omega=\omega_0^+=\sqrt{\Omega^2\sin^2\left(\frac{ka}{2}\right)+2\Omega'^2} \qquad (12)$$

These dispersion relations are periodic in wave number, k, with a period of $2\pi/a$ and are represented graphically in the band structure of Fig. 2. The lower band passing by $k=0$ in Fig. 2 corresponds to the lower frequency solution, i.e., ω_0^-. In this case, the two chains vibrate in phase ($A_0=B_0$) and do not interact with each other, resulting in the dispersion relation of an isolated atomic chain. The upper band in Fig. 2 represents the higher frequency solution, i.e., ω_0^+, where the two chains vibrate out of phase ($A_0=-B_0$).

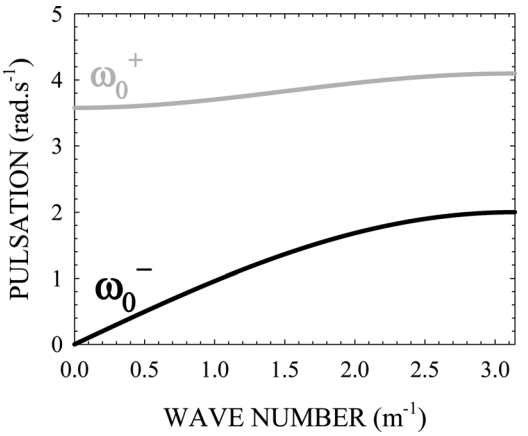

Fig. 2 Band structure associated with the zeroth-order solutions, i.e., $\omega_0^-(k)$ (black line) and $\omega_0^+(k)$ (gray line). Parameters a, m, β, and β' (see text for definitions) were chosen to be $a=1$ m, $m=1$ kg, $\beta=1$ N·m^{-1}, $\beta'=6.4$ N·m^{-1}.

One may write a general solution of Eq. (6) as a superposition of modes corresponding to the lower and upper branches of the band structure

$$\begin{aligned}u_{n,G}^{(0)}=&A_0^+(\tau_1,\tau_2)e^{ikna}e^{-i\omega_0^+\tau_0}+\overline{A_0^+}(\tau_1,\tau_2)e^{-ikna}e^{i\omega_0^+\tau_0}\\ &+A_0^-(\tau_1,\tau_2)e^{ikna}e^{-i\omega_0^-\tau_0}+\overline{A_0^-}(\tau_1,\tau_2)e^{-ikna}e^{+i\omega_0^-\tau_0}\end{aligned} \qquad (13)$$

$$\begin{aligned}v_{n,G}^{(0)}=&-A_0^+(\tau_1,\tau_2)e^{ikna}e^{-i\omega_0^+\tau_0}-\overline{A_0^+}(\tau_1,\tau_2)e^{-ikna}e^{i\omega_0^+\tau_0}\\ &+A_0^-(\tau_1,\tau_2)e^{ikna}e^{-i\omega_0^-\tau_0}+\overline{A_0^-}(\tau_1,\tau_2)e^{-ikna}e^{+i\omega_0^-\tau_0}\end{aligned} \qquad (14)$$

where

$$\begin{cases}A_0^+(\tau_1,\tau_2)=\alpha_0^+(\tau_1,\tau_2)e^{-i\varphi_0^+(\tau_1,\tau_2)}\\ A_0^-(\tau_1,\tau_2)=\alpha_0^-(\tau_1,\tau_2)e^{-i\varphi_0^-(\tau_1,\tau_2)}\end{cases} \qquad (15)$$

$A_0^\pm(\tau_1,\tau_2)$ are complex quantities that permit slow time evolution of amplitude and phase, and $\alpha_0^\pm(\tau_1,\tau_2)$ and $\varphi_0^\pm(\tau_1,\tau_2)$ are real-valued functions. In Eqs. (13) and (14), $\overline{X}$ means complex conjugate of X.

3.2 First-Order Solutions. Equations (13) and (14) are now inserted in the ε^1-order equations (Eq. (7)) to resolve the general solutions for $u_n^{(1)}$ and $v_n^{(1)}$. However, one observes that the right-

hand side (RHS) of Eq. (7*a*) only depends on $u_n^{(0)}$ and includes a second-order derivative of $u_n^{(0)}$ with respect to τ_0 and τ_1. Substituting Eq. (13) in Eq. (7*a*), the RHS of Eq. (7*a*) exhibits terms of the forms $i\omega_0^+(\partial A_0^+(\tau_1,\tau_2)/\partial\tau_1)\,e^{-i\omega_0^+\tau_0}$, $i\omega_0^-(\partial A_0^-(\tau_1,\tau_2)/\partial\tau_1)\,e^{-i\omega_0^-\tau_0}$, and their complex conjugates. It is assumed that the solution to the homogeneous equation of Eq. (7*a*) takes similar form to the general solution of Eq. (6). Under this assumption and to ensure that there are no secular terms (i.e., terms that grow with time and that are incompatible with the assumption that $u_n^{(1)}$ must be a correction to $u_n^{(0)}$) in the particular solution of Eq. (7*a*), the prefactors of $e^{\pm i\omega_0^+\tau_0}$ and $e^{\pm i\omega_0^-\tau_0}$ in the RHS of Eq. (7*a*) are forced to be zero [13,19,20]. Subsequently, the derivatives of the amplitudes A_0^+ and A_0^- with respect to τ_1 must vanish and these amplitudes only depend on τ_2. The same result should be obtained by considering the first-order equation in ε for displacement v_n, i.e., Eq. (7*a*).

The general solutions of Eq. (7*a*) are the sums of homogeneous solutions and particular solutions. Equation (7) has homogeneous solutions that are isomorphic to Eqs. (13) and (14), where the amplitudes $A_0^{\pm}(\tau_2)$ are replaced by $A_1^{\pm}(\tau_2)$. The second terms in the RHS of Eq. (7) constitute forcing functions at the frequencies $2\omega_0^{\pm}$ and $(\omega_0^+ + \omega_0^-)$. We seek particular solutions in the form

$$\begin{aligned} u_{n,P}^{(1)} = {} & D_1 e^{2ikna} e^{-2i\omega_0^+\tau_0} + D_1' e^{-2ikna} e^{2i\omega_0^+\tau_0} \\ & + E_1 e^{2ikna} e^{-2i\omega_0^-\tau_0} + E_1' e^{-2ikna} e^{2i\omega_0^-\tau_0} \\ & + F_1 e^{2ikna} e^{-i(\omega_0^+ + \omega_0^-)\tau_0} + F_1' e^{-2ikna} e^{i(\omega_0^+ + \omega_0^-)\tau_0} \end{aligned} \tag{16}$$

$$\begin{aligned} v_{n,P}^{(1)} = {} & I_1 e^{2ikna} e^{-2i\omega_0^+\tau_0} + I_1' e^{-2ikna} e^{2i\omega_0^+\tau_0} \\ & + J_1 e^{2ikna} e^{-2i\omega_0^-\tau_0} + J_1' e^{-2ikna} e^{2i\omega_0^-\tau_0} \\ & + K_1 e^{2ikna} e^{-i(\omega_0^+ + \omega_0^-)\tau_0} + K_1' e^{-2ikna} e^{i(\omega_0^+ + \omega_0^-)\tau_0} \end{aligned} \tag{17}$$

One finds

$$D_1 = \frac{-2i(\sin(2ka) - 2\sin(ka))}{m} \cdot \Phi_1(2\omega_0^+) \cdot A_0^{+2} \tag{18}$$

$$D_1' = \frac{2i(\sin(2ka) - 2\sin(ka))}{m} \cdot \Phi_1(2\omega_0^+) \cdot \overline{A_0^+}^2 \tag{19}$$

$$E_1 = \frac{-2i(\sin(2ka) - 2\sin(ka))}{m} \cdot \Phi_1(2\omega_0^-) \cdot A_0^{-2} \tag{20}$$

$$E_1' = \frac{2i(\sin(2ka) - 2\sin(ka))}{m} \cdot \Phi_1(2\omega_0^-) \cdot \overline{A_0^-}^2 \tag{21}$$

$$F_1 = \frac{-4i(\sin(2ka) - 2\sin(ka))}{m} \cdot \Phi_3(\omega_0^+ + \omega_0^-) \cdot A_0^+ \cdot A_0^- \tag{22}$$

$$F_1' = \frac{4i(\sin(2ka) - 2\sin(ka))}{m} \cdot \Phi_3(\omega_0^+ + \omega_0^-)\overline{A_0^+}\,\overline{A_0^-} \tag{23}$$

$$I_1 = \frac{-2i(\sin(2ka) - 2\sin(ka))}{m} \cdot \Phi_2(2\omega_0^+) \cdot A_0^{+2} \tag{24}$$

$$I_1' = \frac{2i(\sin(2ka) - 2\sin(ka))}{m} \cdot \Phi_2(2\omega_0^+) \cdot \overline{A_0^+}^2 \tag{25}$$

$$J_1 = \frac{-2i(\sin(2ka) - 2\sin(ka))}{m} \cdot \Phi_2(2\omega_0^-) \cdot A_0^{-2} \tag{26}$$

$$J_1' = \frac{2i(\sin(2ka) - 2\sin(ka))}{m} \cdot \Phi_2(2\omega_0^-) \cdot \overline{A_0^-}^2 \tag{27}$$

$$K_1 = \frac{4i(\sin(2ka) - 2\sin(ka))}{m} \cdot \Phi_4(\omega_0^+ + \omega_0^-) \cdot A_0^+ A_0^- \tag{28}$$

$$K_1' = \frac{-4i(\sin(2ka) - 2\sin(ka))}{m} \cdot \Phi_4(\omega_0^+ + \omega_0^-)\overline{A_0^+}\,\overline{A_0^-} \tag{29}$$

where

$$\Phi_1(\omega) = \frac{\delta(\omega^2 - \Omega^2\sin^2(ka) - \Omega'^2) - \Omega'^2}{(\omega^2 - \Omega^2\sin^2(ka) - 2\Omega'^2)(\omega^2 - \Omega^2\sin^2(ka))} \tag{30}$$

$$\Phi_2(\omega) = \frac{(\omega^2 - \Omega^2\sin^2(ka) - \Omega'^2) - \delta\Omega'^2}{(\omega^2 - \Omega^2\sin^2(ka) - 2\Omega'^2)(\omega^2 - \Omega^2\sin^2(ka))} \tag{31}$$

$$\Phi_3(\omega) = \frac{\delta(\omega^2 - \Omega^2\sin^2(ka) - \Omega'^2) + \Omega'^2}{(\omega^2 - \Omega^2\sin^2(ka) - 2\Omega'^2)(\omega^2 - \Omega^2\sin^2(ka))} \tag{32}$$

$$\Phi_4(\omega) = \frac{(\omega^2 - \Omega^2\sin^2(ka) - \Omega'^2) + \delta\Omega'^2}{(\omega^2 - \Omega^2\sin^2(ka) - 2\Omega'^2)(\omega^2 - \Omega^2\sin^2(ka))} \tag{33}$$

The functions Φ_1, Φ_2, Φ_3, and Φ_4 may be singular and contain information about the resonant processes that underlie the nonlinear modes of our system.

3.3 Second-Order Solutions. The first-order solutions are now inserted into Eq. (8). Since zeroth- and first-order solutions are independent of τ_1, the first and third terms in the RHS of Eq. (8) vanish. Some of the terms in the square brackets lead to forcing functions in $e^{\pm i\omega_0^{\pm}}$. This results in secular terms that need to be canceled by the second term in the RHS of Eq. (8). After several algebraic steps, we find that $\varphi_0^-(\tau_2)$ and $\varphi_0^+(\tau_2)$ are linear functions of τ_2. Equation (8*a*) leads to corrections to the frequencies of the zeroth-order lower and upper branches

$$\begin{aligned} \omega^+ = {} & \omega_0^+ + \frac{4\delta(\sin(2ka) - 2\sin(ka))^2}{\omega_0^+ m^2} \\ & \times \varepsilon^2\left[\alpha_0^{+2}\Phi_1(2\omega_0^+) + 2\alpha_0^{-2}\Phi_3(\omega_0^+ + \omega_0^-)\right] \end{aligned} \tag{34}$$

$$\begin{aligned} \omega^- = {} & \omega_0^- + \frac{4\delta(\sin(2ka) - 2\sin(ka))^2}{\omega_0^- m^2} \\ & \times \varepsilon^2\left[\alpha_0^{-2}\Phi_1(2\omega_0^-) + 2\alpha_0^{+2}\Phi_3(\omega_0^+ + \omega_0^-)\right] \end{aligned} \tag{35}$$

and Eq. (8*b*) leads to the corrections

$$\begin{aligned} \omega^+ = {} & \omega_0^+ + \frac{4(\sin(2ka) - 2\sin(ka))^2}{\omega_0^+ m^2} \\ & \times \varepsilon^2\left[\alpha_0^{+2}\Phi_2(2\omega_0^+) + 2\alpha_0^{-2}\Phi_4(\omega_0^+ + \omega_0^-)\right] \end{aligned} \tag{36}$$

$$\begin{aligned} \omega^- = {} & \omega_0^- + \frac{4(\sin(2ka) - 2\sin(ka))^2}{\omega_0^- m^2} \\ & \times \varepsilon^2\left[\alpha_0^{-2}\Phi_2(2\omega_0^-) + 2\alpha_0^{+2}\Phi_4(\omega_0^+ + \omega_0^-)\right] \end{aligned} \tag{37}$$

In the case of the nonlinear–nonlinear two-chain model, $\delta = 1$, and $\Phi_1 = \Phi_2$ and $\Phi_3 = \Phi_4$. Equations (34) and (35) and Eqs. (36) and (37) become identical. These functions do not exhibit singularities that are the signature of resonances. In the case of the linear–nonlinear model, $\delta = 0$, the set of Eqs. (34) and (35) does not lead to corrections to the band structure. Only Eqs. (36) and (37) result in second-order frequency shifts. The functions $\Phi_2(2\omega_0^+)$ and $\Phi_4(\omega_0^+ + \omega_0^-)$ have no poles. A resonance appears

due to the singularity of the function $\Phi_2(2\omega_0^-)$ at some nonvanishing specific value of the wave number, $k = k_c$. Therefore, the self-interaction results in a resonance for $k = k_c$. The condition of resonance is

$$4\omega_0^{-2}(k_c) - \Omega^2 \sin^2(k_c a) - 2\Omega'^2 = 0 \tag{38}$$

which is equivalent to

$$4\omega_0^{-2}(k_c) - \omega_0^{+2}(2k_c) = 0 \tag{39}$$

From Eqs. (38) and (11), one obtains k_c as

$$k_c = \pm \frac{2}{a} \arcsin\left[\left(\frac{\Omega'^2}{2\Omega^2}\right)^{\frac{1}{4}}\right] \tag{40}$$

and one notes that k_c depends on the ratio Ω'/Ω.

In Fig. 3, we plot the corrected frequencies in the case $\delta = 0$ (linear–nonlinear system). This resonance occurs between two modes in the lower band and one mode in the upper band. We note that if $k_c > 0$ and $2k_c$ lies outside the first Brillouin zone of the system, then the upper branch phonon associated with the resonance will be located at $(2\pi/a) - 2k_c$. If $k_c < 0$ and $2k_c$ is outside the first Brillouin zone, then the upper branch resonant phonon occurs at $2k_c - (2\pi/a)$.

Figure 3 illustrates the effect of the magnitude of the spring constant coupling the chains. Even though these coupling springs are linear, they influence the location of the self-interaction resonance. As the strength of the coupling spring constant increases, the value of the critical wave number, k_c, in the positive half of the first Brillouin zone varies from the origin to π/a. We also note that as the wave number approaches k_c from below, the frequency of the lower branch dips dramatically. The frequency ω^- increases as one approaches k_c from above. It can be noted that in the case of identical nonlinear chains ($\delta = 1$), the LHS of Eq. (38) appears both in the numerator and the denominator of functions Φ_1 and Φ_2. Therefore, the singularity disappears and no resonance effect is observed in the band structure.

In summary, we have shown with the help of analytical calculations that when one chain is linear and the other is nonlinear, the two-chain model exhibits a nonlinear resonance near a critical wave number due to mode self-interaction. The existence of such resonance is clearly stated in Eq. (37). This resonance occurs between two phonons in the lower band (passing by $k = 0$) and one phonon in the upper band in the band structure of the two coupled chains.

Moreover, one may analyze the influence of damping inside the coupled atomic chains on the resonance phenomenon by considering complex values (with nonvanishing imaginary part) of β and β'. For the sake of simplicity, we restricted ourselves to the case of damping in the coupling spring β' and we have taken into account a lossy coupling spring with complex stiffness $\beta' = \beta'_r - i\beta'_i$ with $\beta'_i \ll \beta'_r$. To visualize the effect of damping on the resonance, we have chosen to calculate complex eigenfrequencies ω^-, using Eq. (37), for real fixed values of the wave number. In Fig. 4, the computed dispersion curves are reported in the vicinity of k_c when β' takes a complex value with $\beta'_r = 7\ \mathrm{N \cdot m^{-1}}$ and $\beta'_i = 3.5 \times 10^{-2}$, 7×10^{-2}, and $1.4 \times 10^{-1}\ \mathrm{N \cdot m^{-1}}$ (the other parameters are the same as those of Fig. 3(*c*)). Comparison between Figs. 3(*c*) and 4 shows, as expected in such kind of phenomenon [21], that damping in the coupling spring produces a decrease of resonance amplitude and an increase of resonance width proportional to β'_i. From the imaginary part of the eigenfrequencies (see bottom panel of Fig. 4), one may estimate the width at half-maximum Γ of the resonance peak. Values of $\Gamma = 9.5 \times 10^{-3}$, 1.9×10^{-2}, and $3.8 \times 10^{-2}\ \mathrm{m^{-1}}$ are obtained for $\beta'_i = 3.5 \times 10^{-2}$, 7×10^{-2}, and $1.4 \times 10^{-1}\ \mathrm{N \cdot m^{-1}}$, respectively. Parameter Γ can be calculated analytically with the help of the acoustic resonance scattering theory [21]. Indeed, as already mentioned, the resonance phenomenon is associated with the singularity of the function $\Phi_2(2\omega_0^-)$ (see Eq. (31)) for $k = k_c$ and the condition of resonance is given by $D(k) = 4\omega_0^{-2} - \Omega^2 \sin^2(ka) - 2\Omega'^2 = 0$ for $k = k_c$ (see Eq. (38)). In other words, $D(k)$ is a resonant term of the amplitude of the resonance phenomenon. A Taylor's expansion of this term in the vicinity of k_c leads to

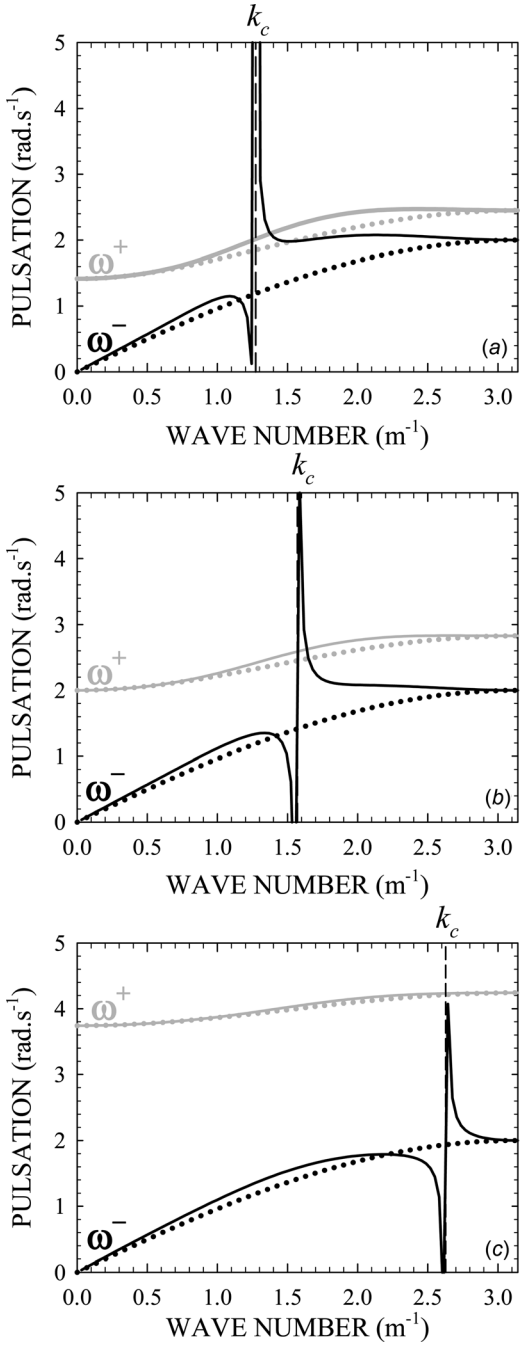

Fig. 3 $\omega^-(k)$ **(black lines) and** $\omega^+(k)$ **(gray lines) as functions of wave number for three values of the spring constant** β'**, namely,** $\beta' = 1\ \mathrm{N \cdot m^{-1}}$ **(*a*),** $2\ \mathrm{N \cdot m^{-1}}$ **(*b*), and** $7\ \mathrm{N \cdot m^{-1}}$ **(*c*). The dotted lines correspond to the linear–linear two-chain model. The system parameters are** $a = 1$ **m,** $m = 1$ **kg,** $\beta = 1\ \mathrm{N \cdot m^{-1}}$**,** $\varepsilon = 1.6\ \mathrm{N \cdot m^{-2}}$**,** $\alpha_0^+ = \alpha_0^- = 0.17$ **m. The black dashed line indicates the value of the critical wave number:** $k_c = 1.27\ \mathrm{m^{-1}}$ **(*a*),** $k_c = 1.57\ \mathrm{m^{-1}}$ **(*b*), and** $k_c = 2.63\ \mathrm{m^{-1}}$ **(*c*).**

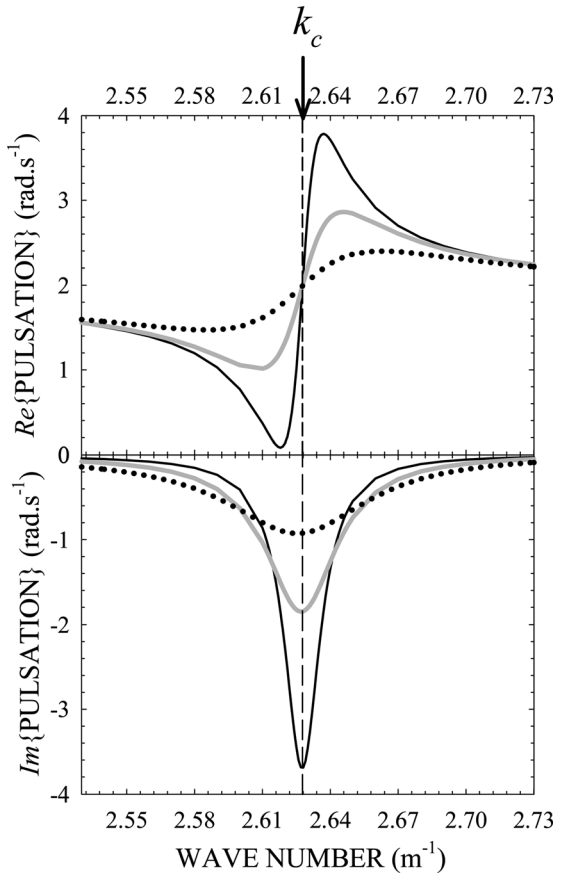

Fig. 4 Complex pulsation ω^- as function of the wave number around the critical wave number k_c when the stiffness β' of the spring coupling together the two horizontal chains takes complex values with real part equals to 7 N · m^{-1} and imaginary part equals to 3.5×10^{-2} N · m^{-1} (black solid lines), 7.0×10^{-2} N · m^{-1} (gray solid lines), and 1.4×10^{-1} N · m^{-1} (black dotted lines). The top (resp. bottom) panel represents the behavior of the real (resp. imaginary) part of the pulsation ω^-. The other parameters are the same as those of Fig. 3(c). The black dashed line indicates the value of the critical wave number: $k_c = 2.63$ m^{-1}.

$$D(k) \simeq 2\Omega^2 a \sin(k_c a)(1-\cos(k_c a)) \times \left[(k-k_c) + i\frac{\beta'_i}{m\Omega^2 a \cdot \sin(k_c a)\cdot(1-\cos(k_c a))}\right]$$

One may verify, according to the acoustic resonance scattering theory [21] that the imaginary part of the quantity appearing in square brackets is equal to half of the parameter Γ, i.e., $\Gamma = (2\beta'_i/m\Omega^2 a \cdot \sin(k_c a)\cdot(1-\cos(k_c a)))$. One may check easily that values of Γ deduced from Fig. 4 are in excellent agreement with this analytical expression. Finally, effect of damping inside the coupled atomic chains on the observed resonance was predictable and does not influence drastically the phenomenon in the limit of small damping, i.e., for $\beta'_i \ll \beta'_r$.

3.4 Energy Transfer in the Linear–Nonlinear Two-Chain Model. We investigate now the possibility of energy transfer in the linear–nonlinear two-chain model. The total energy is expressed as the sum of the quadratic kinetic energy (T) and quadratic potential energy of each chain (U), the quadratic energy associated with the coupling between chains (U_c), and a source of nonlinearity taking the form of a cubic term for one of the chains proportional to ε (U_{NL})

$$E = T + U + U_c + U_{NL} = \frac{1}{2}m\sum_n \left[\dot{u}_n\dot{\overline{u}}_n + \dot{v}_n\dot{\overline{v}}_n\right] + \frac{1}{2}\beta\sum_n (u_{n+1}-u_n)(\overline{u}_{n+1}-\overline{u}_n) + \frac{1}{2}\beta\sum_n (v_{n+1}-v_n)(\overline{v}_{n+1}-\overline{v}_n) + \frac{1}{2}\beta'\sum_n (u_n-v_n)(\overline{u}_n-\overline{v}_n) + \frac{1}{3}\varepsilon\sum_n |v_{n+1}-v_n|^2(v_{n+1}-v_n) \quad (41)$$

While the calculation of the total energy is out of reach, we can estimate the contribution of the resonant zeroth-order displacements to the energy of the system. For this, we insert the polynomial series given by Eqs. (4) and (5) into Eq. (41) and neglect all terms in ε, ε^2, and higher powers of ε which include first- and higher-order displacements. We obtain an expression that involves only the zeroth-order solutions: $u_n^{(0)}(t)$ and $v_n^{(0)}(t)$. However, to account for the nonlinear behavior of the model, we employ a superposition of zeroth-order displacements in the lower and upper dispersion branches with the second-order corrected frequency of Eqs. (36) and (37)

$$u_n^{(0)}(t) = \sum_k \left\{C^+(k)e^{ikna}e^{-i\omega^+ t} + \overline{C^+}(k)e^{-ikna}e^{i\omega^+ t} + C^-(k)e^{ikna}e^{-i\omega^- t} + \overline{C^-}(k)e^{-ikna}e^{+i\omega^- t}\right\} \quad (42)$$

$$v_n^{(0)}(t) = \sum_k \left\{-C^+(k)e^{ikna}e^{-i\omega^+ t} - \overline{C^+}(k)e^{-ikna}e^{i\omega^+ t} + C^-(k)e^{ikna}e^{-i\omega^- t} + \overline{C^-}(k)e^{-ikna}e^{+i\omega^- t}\right\} \quad (43)$$

In this form, the effect of the self-interaction is embedded in the frequencies $\omega^+(k)$ and $\omega^-(k)$.

After numerous algebraic steps, we obtain

$$T = \sum_k T(k) = \sum_k \left[m(\omega^-)^2|C^-(k)|^2(2-2\cos(2\omega^- t)) + m(\omega^+)^2|C^+(k)|^2(2-2\cos(2\omega^+ t))\right] \quad (44)$$

$$U = \sum_k U(k) = \sum_k 4\beta\sin^2\left(\frac{ka}{2}\right)\left[|C^-(k)|^2(2+2\cos(2\omega^- t)) + |C^+(k)|^2(2+2\cos(2\omega^+ t))\right] \quad (45)$$

$$U_c = \sum_k U_c(k) = \sum_k 2\beta'|C^+(k)|^2(2+2\cos(2\omega^+ t)) \quad (46)$$

and

$$U_{NL} = \frac{1}{3}\varepsilon\sum_n \left|v_{n+1}^{(0)} - v_n^{(0)}\right|^2\left(v_{n+1}^{(0)} - v_n^{(0)}\right) \quad (47)$$

We verify that when $\omega^\pm = \omega_0^\pm$ and $\varepsilon = 0$, i.e., in the limit of the linear system, the energy may be written as

$$E_0 = E_0^- + E_0^+ \quad (48)$$

with the contribution from the linear lower and upper branches to the energy given by

$$E_0^- = \sum_k E_0^-(k) = \sum_k 16\beta |C^-(k)|^2 \sin^2\left(\frac{ka}{2}\right) \tag{49}$$

$$E_0^+ = \sum_k E_0^+(k) = \sum_k |C^+(k)|^2 \left[16\beta \sin^2\left(\frac{ka}{2}\right) + 4\beta'\right] \tag{50}$$

The energy is independent of time as expected.

Equation (44) includes the nonlinear resonance through the terms $(\omega^-)^2$ and $(\omega^+)^2$ in the kinetic energy. Although the nonlinear energy U_{NL} is first-order in ε and the kinetic energy incorporates only second-order powers of ε, the resonant form of the frequency in Eq. (44) enables us to neglect the nonresonant zeroth-order nonlinear term given by Eq. (47).

Under this condition, for a given wave number, the contribution of the zeroth-order solution with nonlinear correction due to self-interaction is simplified to

$$E(k) = T(k) + U(k) + U_c(k) = E^-(k) + E^+(k) \tag{51}$$

We regroup the terms into the respective contributions from the lower and upper branches $E^-(k)$ and $E^+(k)$. These contributions are functions of time. We, therefore, take the time average of Eq. (51). We plot in Fig. 5, the normalized functions $E_0^-(k)$, $E_0^+(k)$, $E^-(k)$, and $E^+(k)$.

Approaching the critical wave number, k_c, from below, and keeping total energy constant, energy is transferred from the upper branch to the lower branch. The inverse phenomenon is observed when approaching k_c from above. We note that in the case of the nonlinear/nonlinear two-chain model, this interband transfer of energy resulting from the self-interaction resonant phenomenon would not occur. One needs the coupling between a linear chain and a nonlinear chain to achieve the selective exchange of energy between the symmetric (lower band) and antisymmetric (upper band) modes of the two-chain system.

4 Three-Wave Interactions

We investigate now the interactions between three phonons with general wave numbers k, k', and k^*. We focus on the linear–nonlinear two-chain model ($\delta = 0$) for which three–phonon resonant processes have been identified through the self-interaction analysis. Specifically, we are interested in identifying

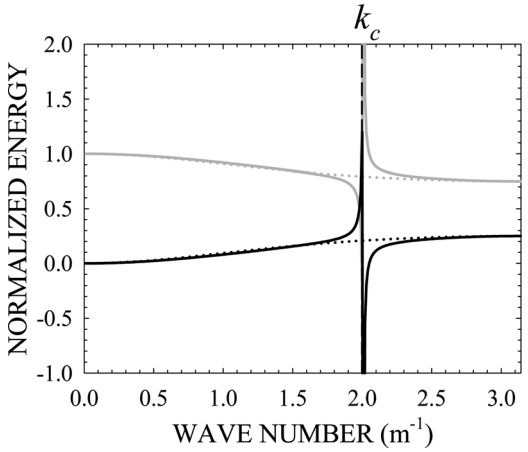

Fig. 5 Contributions of the lower and upper dispersion branches to the energy of the linear two-chain model (dotted lines), $E_0^-(k)$ (black) and $E_0^+(k)$ (gray), and the linear–nonlinear model (solid lines), $E^-(k)$ (black) and $E^+(k)$ (gray) normalized to their respective total energy, $E_0(k)$ and $E(k)$. The system parameters are $a = 1$ m, $m = 1$ kg, $\beta = 1$ N·m^{-1}, $\beta' = 4$ N·m^{-1}, $\varepsilon = 1.6$ N·m^{-2}, $\alpha_0^+ = \alpha_0^- = 0.17$ m. The black dashed line indicates the value of the critical wave number: $k_c = 2.0$ m^{-1}.

nonlinear modes which arise from three-phonon interactions. For this, we need to insert a superposition of zeroth-order solutions into Eq. (7).

Again, we assume that all solutions are independent of τ_1. The time derivatives on the RHS of Eq. (7) vanish. For the linear–nonlinear two-chain system, Eq. (7) takes the simpler form

$$\begin{cases} \dfrac{\partial^2 u_n^{(1)}}{\partial \tau_0^2} - \dfrac{\Omega^2}{4}\left(u_{n+1}^{(1)} - 2u_n^{(1)} + u_{n-1}^{(1)}\right) - \Omega'^2\left(v_n^{(1)} - u_n^{(1)}\right) = 0 \\ \dfrac{\partial^2 v_n^{(1)}}{\partial \tau_0^2} - \dfrac{\Omega^2}{4}\left(v_{n+1}^{(1)} - 2v_n^{(1)} + v_{n-1}^{(1)}\right) + \Omega'^2\left(v_n^{(1)} - u_n^{(1)}\right) \\ = \dfrac{1}{m}\left[\left(v_{n+1}^{(0)} - v_n^{(0)}\right)^2 - \left(v_n^{(0)} - v_{n-1}^{(0)}\right)^2\right] \end{cases} \tag{52}$$

Using the superposition of zeroth-order solutions

$$v_{n,G}^{(0)} = \sum_k \left\{-A_0^+(\tau_2)e^{ikna}e^{-i\omega_0^+\tau_0} - \overline{A_0^+}(\tau_2)e^{-ikna}e^{i\omega_0^+\tau_0} + A_0^-(\tau_2)e^{ikna}e^{-i\omega_0^-\tau_0} + \overline{A_0^-}(\tau_2)e^{-ikna}e^{+i\omega_0^-\tau_0}\right\} \tag{53}$$

the RHS of the above equation produces intraband and interband wave mixing. In light of the origin of the self-interaction resonances, we pay particular attention to the forcing terms corresponding to the mixing of two modes in the lower band. These are terms proportional to $e^{\pm i(\omega_0^-(k)+\omega_0^-(k'))\tau_0}$. We choose first-order solutions in the form

$$u_n^{(1)} = \sum_k A_1(k,\tau_0,\tau_2)e^{ikna} \tag{54}$$

$$v_n^{(1)} = \sum_k B_1(k,\tau_0,\tau_2)e^{ikna} \tag{55}$$

Equation (52) is multiplied by e^{ik^*na}, and a summation over all n masses is imposed. Equation (52) reduces to

$$\frac{\partial^2 A_1(k^*,\tau_0,\tau_2)}{\partial \tau_0^2} + \Omega^2 A_1(k^*,\tau_0,\tau_2)\sin^2\left(\frac{k^*a}{2}\right) - \Omega'^2[B_1(k^*,\tau_0,\tau_2) - A_1(k^*,\tau_0,\tau_2)] = 0 \tag{56}$$

$$\frac{\partial^2 B_1(k^*,\tau_0,\tau_2)}{\partial \tau_0^2} + \Omega^2 B_1(k^*,\tau_0,\tau_2)\sin^2\left(\frac{k^*a}{2}\right) - \Omega'^2[A_1(k^*,\tau_0,\tau_2) - B_1(k^*,\tau_0,\tau_2)] = \frac{1}{m}\sum_k\sum_{k'} A_0^-(k)A_0^-(k') \times e^{-i\left(\omega_0^-(k)+\omega_0^-(k')\right)\tau_0}\delta_{k^*,k+k'}f(k,k') + \text{other terms} \tag{57}$$

The function f is given by $f(k,k') = (e^{ika} - 1)(e^{ik'a} - 1) - (e^{-ika} - 1)(e^{-ik'a} - 1)$.

The homogeneous solutions of Eqs. (56) and (57) are similar to the zeroth-order solutions. Nonlinear effects are sought in the particular solutions by considering the first-order particular amplitudes in Eqs. (54) and (55) to follow the forcing term in the RHS of Eq. (57). These are

$$A_{1,p}(k^*,\tau_0,\tau_2) = \sum_k\sum_{k'} U_1(k,k',\tau_2)e^{-i(\omega_0^-(k)+\omega_0^-(k'))\tau_0}\delta_{k^*,k+k'}f(k,k') \tag{58}$$

$$B_{1,p}(k^*,\tau_0,\tau_2) = \sum_k\sum_{k'} V_1(k,k',\tau_2)e^{-i(\omega_0^-(k)+\omega_0^-(k'))\tau_0}\delta_{k^*,k+k'}f(k,k') \tag{59}$$

Combining Eqs. (56) and (57) and Eqs. (58) and (59) results in the following amplitudes of the particular solutions:

$$U_1(k,k') = \frac{1}{m} \frac{A_0^-(k)A_0^-(k')\Omega'^2}{\left[-\left(\omega_0^-(k)+\omega_0^-(k')\right)^2 + \Omega^2 \sin^2\left(\frac{k^* a}{2}\right) + \Omega'^2\right]^2 - \Omega'^4} \tag{60}$$

$$V_1(k,k') = \frac{1}{m} \frac{A_0^-(k)A_0^-(k')\left[-\left(\omega_0^-(k)+\omega_0^-(k')\right)^2 + \Omega^2 \sin^2\left(\frac{k^* a}{2}\right) + \Omega'^2\right]}{\left[-\left(\omega_0^-(k)+\omega_0^-(k')\right)^2 + \Omega^2 \sin^2\left(\frac{k^* a}{2}\right) + \Omega'^2\right]^2 - \Omega'^4} \tag{61}$$

with $k^* = k + k'$.

The denominators of Eqs. (60) and (61) present singularities when

$$\left(\omega_0^-(k)+\omega_0^-(k')\right)^2 - \Omega^2 \sin^2\left(\frac{(k+k')a}{2}\right) - 2\Omega'^2 = 0 \tag{62}$$

This condition for resonance can be simplified to

$$(\omega_0^-(k)+\omega_0^-(k'))^2 - (\omega_0^+(k+k'))^2 = 0 \tag{63}$$

Equation (63) generalizes Eq. (39) beyond self-interaction. Indeed, the resonant condition of Eq. (63) is satisfied by considering the self-interaction, $k = k' = k_c$. A similar condition also exists for wave numbers in the negative sector of the Brillouin zone. Equation (63) describes a three-phonon resonant process whereby, two phonons in the lower branch of the band structure of the two-chain system interact to form a phonon in the upper branch. We may also consider first-order solutions in the vicinity of the resonance. For instance, taking $k' = k_c$ with $k \neq k_c$ will lead to first-order solutions, which frequency $\omega_0^-(k) + \omega_0^-(k')$ does not lie on the upper branch of the band structure. The dispersion curve of these nonlinear modes is given by

$$\omega_0^{\mathrm{NL}}(k+k_c) = \omega_0^-(k) + \omega_0^-(k_c) \text{ when } 0 < k < \frac{\pi}{a} \tag{64}$$

and is displayed in Fig. 6. This dispersion curve starts from the linear lower mode at $k_\ell = k_c$ and crosses the upper linear mode at $k_u = (2\pi/a) - 2k_c$. The branch folds when $k + k_c > (\pi/a)$. The amplitude of these nonlinear modes given by Eqs. (60) and (61) will decrease as k deviates away from the critical wave number. Thus, if $k + k_c > (\pi/a)$, no mode will exhibit higher amplitude when $k = k_u$ at the crossing of nonlinear mode and linear upper mode branches.

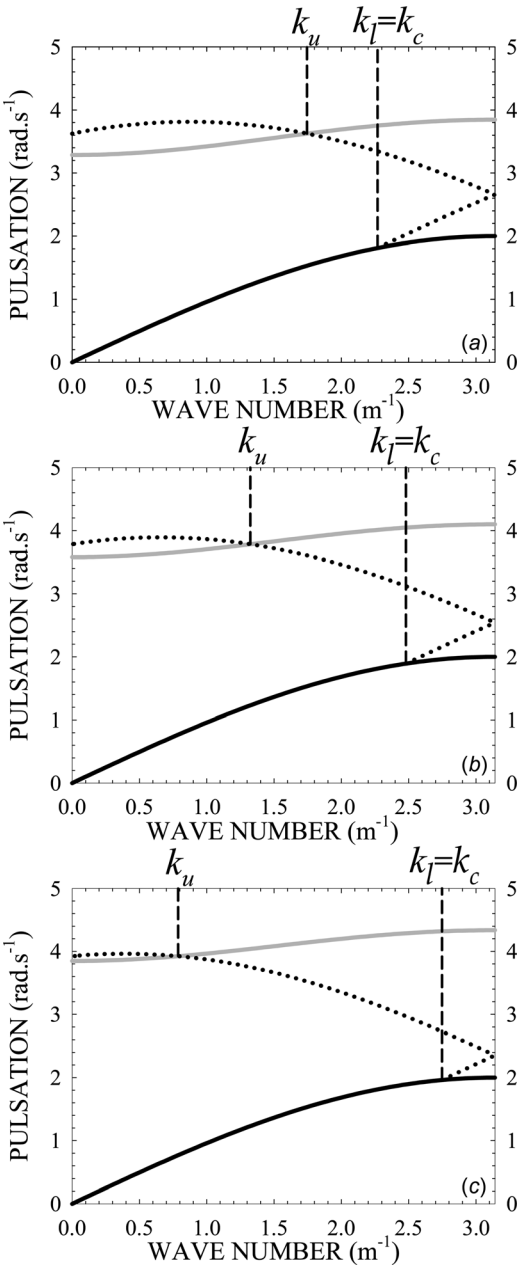

Fig. 6 $\omega_0^-(k)$ (black solid line), $\omega_0^+(k)$ (gray solid line), and $\omega_0^{\mathrm{NL}}(k+k_c) = \omega_0^-(k_c)+\omega_0^-(k)$ (black dotted line) as functions of wave number for three values of the spring constant β', namely, 5.4 N·m^{-1} (*a*), 6.4 N·m^{-1} (*b*), and 7.4 N·m^{-1} (*c*). The system parameters are $a = 1$ m, $m = 1$ kg, $\beta = 1$ N·m^{-1}. $k_\ell = k_c$ and $k_u = (2\pi/a) - 2k_c$ are the wave numbers at which the nonlinear branch (black dotted line) intersects the lower and the upper linear bands. The black dashed lines indicate the values of the wave numbers: $k_\ell = 2.27$ m^{-1} and $k_u = 1.74$ m^{-1} (*a*), $k_\ell = 2.48$ m^{-1} and $k_u = 1.32$ m^{-1} (*b*), and $k_\ell = 2.75$ m^{-1} and $k_u = 0.78$ m^{-1} (*c*).

5 Numerical Results

We employ the method of molecular dynamics [22] to calculate the distribution of phonons under conditions of thermal equilibrium in the linear–nonlinear coupled chain system. This approach enables us to investigate this system beyond the limit of perturbation theory. We consider a system composed of two chains, each containing $N = 800$ masses. The parameters of the system are $a = 1$ m, $m = 1$ kg, $\beta = 1$ N·m^{-1}, and $\varepsilon = 1.6$ N·m^{-2}. Periodic boundary conditions are employed to mimic the behavior of an infinite system. A random distribution of mass displacements is used as initial condition, and trajectories of the masses are numerically integrated under constant energy conditions. The velocity of each mass is recorded during the whole length of the simulation which amounts to 2^{21} integration steps ($\Delta t = 2.5$ ms). These velocities are then utilized to calculate the SED of phonons in the space (k, ω). This method is described in Ref. [23] and has been successfully applied to the study of phonon scattering in single one-dimensional (1D) anharmonic atomic chains [20]. In Fig. 7, we report the SED results for three values of the elastic constant of the spring coupling the two chains, $\beta' = 5.4$, 6.4, and 7.4 N·m^{-1}. The vibrational modes with the highest SED values describe quite well the two bands constituting the band structure of the linear system, i.e., $\omega_0^-(k)$ and $\omega_0^+(k)$ (see Fig. 2 and Sec. 3.1). Signature of the self-interaction resonance appears in the presence of a folded nonlinear dispersion branch that connects

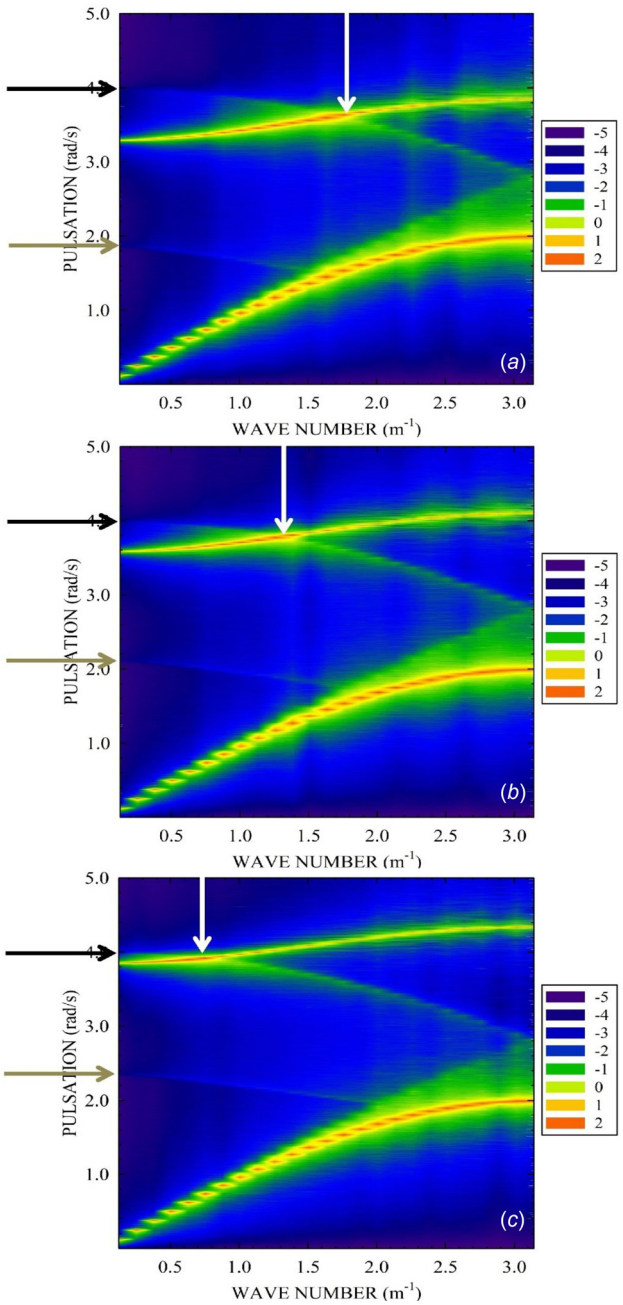

Fig. 7 SEDs in J.s calculated from the velocities of the atoms in the linear–nonlinear two chains model for three values of the coupling elastic constant $\beta' = 5.4\ \mathrm{N \cdot m^{-1}}$ (*a*), $\beta' = 6.4\ \mathrm{N \cdot m^{-1}}$ (*b*), and $\beta' = 7.4\ \mathrm{N \cdot m^{-1}}$ (*c*). The system parameters are $a = 1\ \mathrm{m}$, $\mathrm{m} = 1\ \mathrm{kg}$, $\beta = 1\ \mathrm{N \cdot m^{-1}}$, $\varepsilon = 1.6\ \mathrm{N \cdot m^{-2}}$, $\alpha_0^+ = \alpha_0^- = 0.17\ \mathrm{m}$. The background scale corresponds to $\log_{10}(\mathrm{SED})$. The white arrow indicates the value of k_u^{SED}: $k_u^{\mathrm{SED}} \approx 1.7\ \mathrm{m^{-1}}$ (*a*), $k_u^{\mathrm{SED}} \approx 1.3\ \mathrm{m^{-1}}$ (*b*), and $k_u^{\mathrm{SED}} \approx 0.7\ \mathrm{m^{-1}}$ (*c*). Meaning of the black and gray arrows is given in the text.

the upper and the lower dispersion curves. Indeed, this additional branch disappears in the SED calculation of the band structure of the nonlinear–nonlinear two-chain system (not reported) where self-interaction resonance does not occur. One notes that the nonlinear band calculated with the SED method has almost the same characteristics as those of the first-order modes in the vicinity of the resonant three-phonon process determined in Sec. 4 (see Fig. 6). Especially, this band after folding at the border of the irreducible Brillouin zone (at $k = \pi/a$) intersects the upper linear band for a wave number, k_u^{SED}, very close to k_u determined analytically in Sec. 4. As predicted analytically, k_u^{SED} shifts toward the origin of the band structure as β' increases. Beyond the intersection point, other nonlinear modes (shown with the black arrow in Fig. 7) with much lower amplitude occur, as expected in Fig. 6. Again, the nonlinear band is formed of modes that have wave vector $k + k_c$ and frequencies $\omega_0^-(k) + \omega_0^-(k_c)$. Nevertheless, in Fig. 7, additional modes appear, especially around the lower linear band. In this range of frequency, it seems that each nondegenerate wave vector is associated with multiple eigenfrequencies and the number of these eigenfrequency increases when the wave number approaches the edge of the irreducible Brillouin zone. A similar phenomenon was already observed in the framework of three-phonon scattering processes in 1D anharmonic monoatomic crystals [20]. Equations (60) and (61) of Sec. 4 are utilized to explain the appearance of these additional modes. These equations represent the first-order term in the asymptotic expansion of $A_{1,p}(k^*, \tau_0, \tau_2)$ and $B_{1,p}(k^*, \tau_0, \tau_2)$, describing three-wave interactions. Inside the double summation over (k', k'') in Eqs. (58) and (59), conservation of wave vectors is imposed: $\delta_{k^*,k'+k''} \to k^* = k' + k''$. If the mode of interest is $k^* = \pi/a$, then conservation of wave vector can be satisfied by adding nondegenerate wave vector pairs that yield k^*. However, such combination of wave vectors does not conserve frequency. Indeed, since the dispersion relationship for 1D anharmonic monoatomic chain is not strictly linear, the frequency of mode k' plus (or minus) the frequency of mode k'' will not exactly equal the frequency of mode $k^* = k' + k''$. Instead, the addition (or subtraction) of the frequencies associated with modes k' and k'' will be slightly greater than (or less than) the frequency of mode k^*. This forces the denominator of the pre-exponential factors in Eqs. (58) and (59) to become small, thereby contributing to a large value of U_1 and V_1. These additional modes combine only modes of the lower branch and are nearly independent of β' as it can be observed in Fig. 7. As a matter of results, the effect of β' on the intersection point between the nonlinear band and the lower linear band (named as k_ℓ in Sec. 4) cannot be clearly observed because the classical three-phonon interactions in the lower band overwhelm the three-phonon interband nonlinear interaction. For the same reason, it is difficult to define exactly the frequency at which the nonlinear band is folded at the edge of the irreducible Brillouin zone, i.e., for $k = \pi/a$. Finally, the gray arrows in Fig. 7 show vibrational modes starting at the center of the Brillouin zone and exhibiting a negative dispersion. Pulsations of these modes slightly depend on β'. The SED of these modes is at least ten times lower than that of the nonlinear modes connecting the lower and upper linear bands and this very low value of the SED indicates that they might correspond to higher-order nonlinear modes.

6 Conclusions

We have used multiple-time-scales perturbation theory as well as the numerical methods of molecular dynamics and SED to investigate the band structure of a two-chain model with anharmonic interactions. We have considered the case of second-order nonlinear chains coupled via a linear spring as well as one linear chain coupled linearly to a second-order nonlinear chain. The linear–nonlinear two-chain model exhibits a nonlinear effect whereby modes near a critical wave number resonate through self-interaction. The resonance can be tuned by changing the spring constant of the linear spring connecting the two chains. The nonlinear resonance enables wave number-dependent interband energy transfer between the symmetric and asymmetric modes of the linear–nonlinear two-chain model. This system may be applied to targeted irreversible energy transfer of undesirable mechanical wave energy that could absorb the energy through additional dissipative mechanisms. In contrast, the nonlinear–nonlinear model does not possess such a resonance. We have also demonstrated in the case of the second-order linear–nonlinear two-chain model that there exist nonlinear modes within the spectral gap separating the lower asymmetric and upper symmetric

branches of the phonon band structure. These modes result from the interaction between a phonon belonging to the nonlinear branch and two phonons lying on the lower branch. When stimulated at a frequency corresponding to a nonlinear mode, this linear–nonlinear system may, therefore, be used to split a phonon into a pair of phonons. The two phonons in the lower branch have a combined frequency and wave number equal to the frequency and wave number of the nonlinear phonon. The amplitude of the two emitted phonons depends on their spectral proximity to a critical wave number, k_c, corresponding to a self-interaction resonance. These nonlinear modes may serve as a source of two correlated phonons provided the split phonons are phase-matched in the frequency domain. Such two-photon sources in second-order nonlinear photonic materials or even three-photon sources in third-order nonlinear materials have been described [24,25]. The present study offers an avenue to achieve similar type of phenomena with phonons instead of photons.

Acknowledgment

B. Dubus and P. A. Deymier acknowledge the CNRS Laboratoire International Associé "*Matériaux et Optique*" (MATEO) which supported exchange visits in their respective laboratories.

References

[1] Vakakis, A. F., Gendelman, O. V., Bergman, L. A., McFarland, D. M., Kerschen, G., and Lee, Y. S., 2009, *Nonlinear Targeted Energy Transfer in Mechanical and Structural Systems* (Solid Mechanics and Its Application), Springer, Dordrecht, The Netherlands.

[2] Vakakis, A. F., and Rand, R. H., 2004, "Nonlinear Dynamics of a System of Coupled Oscillators With Essential Stiffness Nonlinearity," Int. J. Nonlinear Mech., **39**(7), p. 1079.

[3] Gendelman, O. V., Sapsis, T., Vakakis, A. F., and Bergman, L. A., 2011, "Enhanced Passive Targeted Energy Transfer in Strongly Nonlinear Mechanical Oscillators," J. Sound Vib., **330**(1), pp. 1–8.

[4] Gendelman, O. V., Manevitch, L. I., Vakakis, A. F., and M'Closkey, R., 2001, "Energy Pumping in Nonlinear Mechanical Oscillators: Part I-Dynamics of the Underlying Hamiltonian System," Trans. ASME, **68**(1), pp. 34–41.

[5] Kerschen, G., Vakakis, A. F., Lee, Y. S., McFarland, D. M., Kowtko, J. J., and Bergman, L. A., 2005, "Energy Transfer in a System of Two Coupled Oscillators With Essential Nonlinearity: 1:1 Resonance Manifold and Transient Bridging Orbits," Nonlinear Dyn., **42**(3), pp. 283–303.

[6] Laxalde, D., Thouverez, F., and Simou, J.-J., 2006, "Dynamics of a Linear Oscillator Connected to a Small Strongly Nonlinear Hysteretic Absorber," Int. J. Nonlinear Mech., **41**(8), pp. 969–978.

[7] Panagopoulos, P. N., Vakakis, A. F., and Tsakirtzis, S., 2004, "Transient Resonant Interactions of Finite Linear Chains With Essential Nonlinear End Attachments Leading to Passive Energy Pumping," Int. J. Solids Struct., **41**(22), pp. 6505–6528.

[8] Vakakis, A. F., Manevitch, L. I., Gendelman, O., and Bergman, L., 2003, "Dynamics of Linear Discrete Systems Connected to Local Essential Nonlinear Attachments," J. Sound Vib., **264**(3), pp. 559–577.

[9] Starosvetsky, Y., Hasan, M. A., Vakakis, A. F., and Manevitch, L. I., 2012, "Strongly Nonlinear Beat Phenomena and Energy Exchanges in Weakly Coupled Granular Chains on Elastic Foundations," SIAM J. Appl. Math., **72**(1), pp. 337–361.

[10] Seidel, A., Lin, H. H., and Lee, D. H., 2005, "Phonons in Hubbard Ladders Studied Within the Framework of the One-Loop Renormalization," Phys. Rev. B, **71**(22), p. 22050.

[11] Peyrard, M., and Bishop, A. R., 1989, "Statistical Mechanics of a Nonlinear Model for DNA Denaturation," Phys. Rev. Lett., **62**(23), pp. 2755–2758.

[12] Bender, C. M., and Orszag, S. A., 1999, *Advanced Mathematical Methods for Scientists and Engineers I, Asymptotic Methods and Perturbation Theory*, Springer-Verlag, New York.

[13] Kevorkian, J., and Cole, J. D., 1996, *Scale and Singular Perturbation Methods*, Springer-Verlag, New York.

[14] Belhaq, M., Clerc, R. L., and Hartmann, C., 1988, "Multiple Scales Methods for Finding Invariant Solutions of Two Dimensional Maps and Application," Mech. Res. Commun., **15**(6), p. 361.

[15] Maccari, A., 1999, "A Perturbation Method for Nonlinear Two Dimensional Maps," Nonlinear Dyn., **19**(4), pp. 295–312.

[16] van Horssen, W. T., and ter Brake, M. C., 2009, "On the Multiple Scales Perturbation Method for Difference Equations," Nonlinear Dyn., **55**(4), pp. 401–418.

[17] Helleman, R. H. G., and Montroll, E. W., 1974, "On a Nonlinear Perturbation Theory Without Secular Terms," Physica, **74**(1), pp. 22–74.

[18] Lee, P. S., Lee, Y. C., and Chang, C. T., 1973, "Multiple-Time-Scale Analysis of Spontaneous Radiation Processes. I. One- and Two-Particle Systems," Phys. Rev. A, **8**(4), p. 1722.

[19] Khoo, I. C., and Wang, Y. K., 1976, "Multiple Time Scale Analysis of an Anharmonic Crystal," J. Math. Phys., **17**(2), p. 222.

[20] Swinteck, N., Muralidharan, K., and Deymier, P. A., 2013, "Phonon Scattering in One-Dimensional Anharmonic Crystals and Superlattices: Analytical and Numerical Study," ASME J. Vib. Acoust., **135**(4), p. 041016.

[21] Überall, H., 1992, *Acoustic Resonance Scattering*, Gordon and Breach Science Publishers, Philadelphia, PA, Chap. 4.

[22] Rapaport, D. C., 1995, *The Art of Molecular Dynamics Simulation*, Cambridge University Press, Cambridge, UK.

[23] Thomas, J. A., Turney, J. E., Iutzi, R. M., Amon, C. H., and McGaughey, A. J. H., 2010, "Predicting Phonon Dispersion Relations and Lifetimes From the Spectral Energy Density," Phys. Rev. B, **81**(8), p. 091411.

[24] Dot, A., Borne, A., Boulanger, B., Segonds, P., Félix, C., Bencheikh, K., and Levenson, J. A., 2012, "Energetic and Spectral Properties of Triple Photon Down Conversion in a Phase-Matched $KTiOPO_4$ Crystal," Opt. Lett., **37**(12), p. 2334.

[25] Boitier, F., Orieux, A., Autebert, C., Lemaître, A., Galopin, E., Manquest, C., Sirtori, C., Favero, I., Leo, G., and Ducci, S., 2014, "Electrically Injected Photon-Pair Source at Room Temperature," Phys. Rev. Lett., **112**(18), p. 183901.